Dendritic cell fate is determined by BCL11A

Gregory C. Ippolito[a,1], Joseph D. Dekker[a,1], Yui-Hsi Wang[b], Bum-Kyu Lee[a], Arthur L. Shaffer III[c], Jian Lin[a], Jason K. Wall[a], Baeck-Seung Lee[a], Louis M. Staudt[c], Yong-Jun Liu[d], Vishwanath R. Iyer[a], and Haley O. Tucker[a,2]

[a]Department of Molecular Biosciences, Institute for Cellular and Molecular Biology, University of Texas at Austin, Austin, TX 78712; [b]Division of Allergy and Immunology, Cincinnati Children's Hospital Medical Center, Cincinnati, OH 44229; [c]Metabolism Branch, Center for Cancer Research, National Cancer Institute, National Institutes of Health, Bethesda, MD 20892; and [d]Baylor Institute for Immunology Research, Dallas, TX 75204

Edited* by Richard A. Flavell, Yale School of Medicine and Howard Hughes Medical Institute, New Haven, CT, and approved February 5, 2014 (received for review October 11, 2013)

The plasmacytoid dendritic cell (pDC) is vital to the coordinated action of innate and adaptive immunity. pDC development has not been unequivocally traced, nor has its transcriptional regulatory network been fully clarified. Here we confirm an essential requirement for the BCL11A transcription factor in fetal pDC development, and demonstrate this lineage-specific requirement in the adult organism. Furthermore, we identify BCL11A gene targets and provide a molecular mechanism for its action in pDC commitment. Embryonic germ-line deletion of *Bcl11a* revealed an absolute cellular, molecular, and functional absence of pDCs in fetal mice. In adults, deletion of *Bcl11a* in hematopoietic stem cells resulted in perturbed yet continued generation of progenitors, loss of downstream pDC and B-cell lineages, and persisting myeloid, conventional dendritic, and T-cell lineages. Challenge with virus resulted in a marked reduction of antiviral response in conditionally deleted adults. Genome-wide analyses of BCL11A DNA binding and expression revealed that BCL11A regulates transcription of E2-2 and other pDC differentiation modulators, including ID2 and MTG16. Our results identify BCL11A as an essential, lineage-specific factor that regulates pDC development, supporting a model wherein differentiation into pDCs represents a primed "default" pathway for common dendritic cell progenitors.

The B-cell chronic lymphocytic leukemia/lymphoma 11A (BCL11A) zinc-finger transcription factor was first discovered as a translocated locus in a lethal pediatric B-cell chronic lymphocytic leukemia (1), and subsequently was identified as a protooncogene implicated in numerous types and subtypes of B-cell malignancies (2, 3). The N-terminal region common to all BCL11A isoforms is evolutionarily conserved and can be used to define a superfamily of transcription factors crucial to the development, differentiation, and malignancy of several hematopoietic lineages (4). In vivo experimentation has confirmed an essential requirement for Bcl11a in B-cell lymphopoiesis (5, 6) and has implicated Bcl11a more broadly in hematopoietic stem cell function and in development of lymphoid lineages (6, 7).

Initially thought to be exclusive to B cells, subsequent observations have demonstrated a wider range of function for BCL11A, and surprisingly high levels of BCL11A transcripts in mouse and human plasmacytoid dendritic cells (pDCs) suggested that BCL11A might also play a key role in the biology of this dendritic cell type (4, 8). Recently, BCL11A's necessity has been specifically confirmed in fetal hematopoietic progenitors, yet its function in the adult organism using conditional knockout models and functional assays has yet to be clarified (9). Ranging from the production of type I IFN (IFN-α) in response to infection by viruses, to the induction of regulatory T cells, or the differentiation of germinal-center B cells into plasma cells—the pDC encompasses a broad range of immune functions and is pivotal to the coordination of innate and adaptive immunity (10–12).

An understanding of the molecular control of pDC lineage determination remains an enigma. Unlike its conventional dendritic cell (cDC) counterpart, the pDC shares perplexing similarities with lymphocytes (particularly B cells), including the transcription of regulatory genes normally invoked during primary lymphocyte development (*BCL11A*, *mb-1/CD79A*, *B220/CD45RA*, *SPIB*, *FOXP1*, *E2-2/TCF4*). In this aspect of its molecular physiology, pDCs resemble B cells more so than cDCs; moreover, the expression of key B-cell genes such as *BCL11A* can be used to distinguish the pDC and cDC dendritic lineages in mice and humans (13).

These features have made it difficult to define pDC lineage affiliation (8, 14–17). One recent breakthrough, however, was the finding that the basic helix–loop–helix (HLH) E-protein, E2-2/TCF4, is an essential and specific transcriptional regulator of pDC development (18). One current model proposes that E2-2 activity maintains the cell fate of mature pDCs through opposition of a "default" pathway that would otherwise lead to cDC fate (19). However, a more recent model has alternatively proposed that pDCs represent the default pathway for common DC precursors (CDPs) (20). Because *BCL11A* was found to be a binding target of E2-2 in the CAL-1 human pDC cell line, the first model has specifically postulated that E2-2 promotes murine pDC commitment in part through Bcl11a-mediated repression of cDC differentiation. However, another member of the E2-2 family of E-proteins, E2A/TCF3, is a critical regulator of B-lymphoid development and differentiation (21), and *Bcl11a* has been identified as a direct target of *E2a* in murine B cells (22).

Inhibitor of DNA binding (ID) proteins are natural dominant-negative HLH proteins, which, by protein–protein heterodimerization with E-proteins, antagonize their ability to fulfill lineage-specific functions by blocking their DNA activity. ID2 and ID3 are two such HLH factors known to influence the differentiation of pDCs, cDCs, and B- and T-lymphoid lineages (23–30). ID interactions

Significance

This work demonstrates a key role of the B lymphocyte transcription factor BCL11A in dendritic cell (DC) development. Two major DC subsets—the plasmacytoid DC (pDC) and the conventional DC (cDC)—are believed to arise from a shared precursor called the common DC progenitor (CDP). Potential precursor differences between cDC and pDC generation might nevertheless remain to be elucidated. Here, we show that mutant mice can generate CDPs and cDCs in the absence of BCL11A, whereas pDCs (and also B cells) are abolished. This study also identifies and validates BCL11A target genes using a variety of techniques, and provides a molecular model for BCL11A activity in the B lymphocyte and pDC lineages.

Author contributions: G.C.I., J.D.D., Y.-H.W., A.L.S., J.K.W., and H.O.T. designed research; G.C.I., J.D.D., Y.-H.W., B.-K.L., A.L.S., J.L., J.K.W., and B.-S.L. performed research; G.C.I., J.D.D., A.L.S., L.M.S., Y.-J.L., V.R.I., and H.O.T. contributed new reagents/analytic tools; G.C.I., J.D.D., Y.-H.W., B.-K.L., A.L.S., J.K.W., and H.O.T. analyzed data; G.C.I., J.D.D., and H.O.T. wrote the paper; and G.C.I. and J.K.W. initiated the project.

The authors declare no conflict of interest.

*This Direct Submission article had a prearranged editor.

Data deposition: The data reported in this paper have been deposited in the Gene Expression Omnibus (GEO) database, www.ncbi.nlm.nih.gov/geo (Chip-seq accession no. GSE55043 and microarray no. GSE55237).

[1]G.C.I. and J.D.D. contributed equally to this work.

[2]To whom correspondence should be addressed. E-mail: haleytucker@austin.utexas.edu.

This article contains supporting information online at www.pnas.org/lookup/suppl/doi:10.1073/pnas.1319228111/-/DCSupplemental.

specifically restrain the transcriptional activity of E-proteins (24, 26, 27, 31) as well as other factors crucial to pDC and B-lymphoid biology, including SPIB and PAX5 (21, 32).

The successive stages of commitment to the DC lineage in bone marrow remain poorly understood and are just beginning to be characterized (20). In this study we demonstrate a requirement in vitro and in vivo for Bcl11a during fetal and adult pDC development in the mouse. Complementary experiments using human cell lines expand these observations made in mice and imply determination of pDC cell fate, in part, by a molecular network comprising BCL11A, ID2, ID3, MTG16, and E2-2/TCF4. Genome-wide ChIP-sequencing (ChIP-seq) revealed BCL11A binding to the promoter and other gene-proximal regions of several other key factors implicated in pDC and lymphoid development, including SPI1, SPIB, IKZF1, and E2A/TCF3. We advance a model that is consistent with existing data demonstrating reliance on additional pDC transcription factors, which postulates that the default pathway of CDP differentiation is to produce pDCs.

Results

Confirmation That Bcl11a-Deficient Fetal Liver and Spleen Is Devoid of pDC. In agreement with previous analyses of conventional *Bcl11a*$^{-/-}$ knockout (KO) mice by Liu et al. (5), we observed an absence of B220^{+} cells in liver and spleen isolated from fetal KO mice (Fig. S1*A*). The loss of B220^{+} cells appeared dose-dependent because *Bcl11a*$^{+/-}$ heterozygotes contained B220^{+} populations intermediate between *Bcl11a*$^{+/+}$ wild-type and *Bcl11a*$^{-/-}$

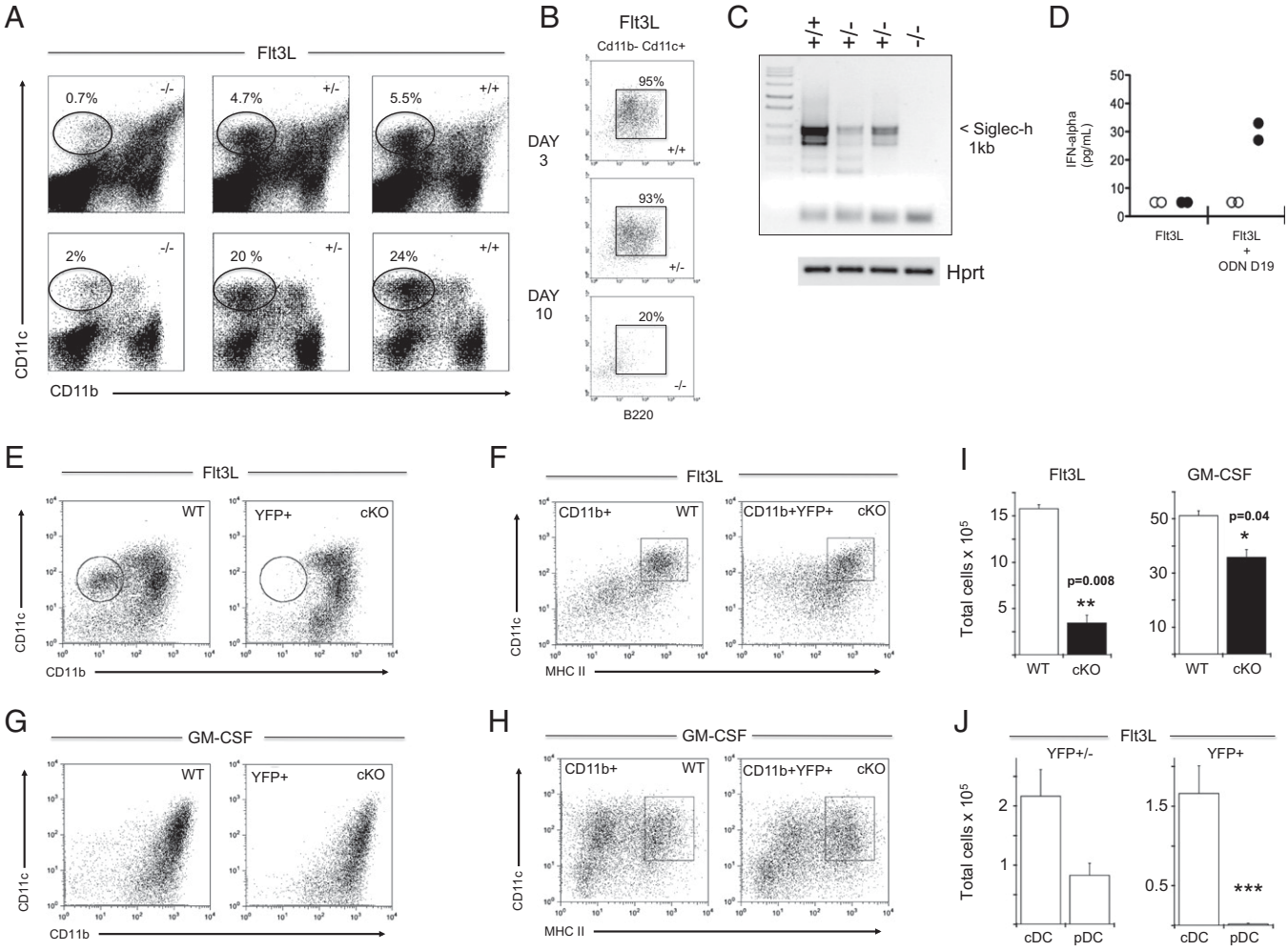

Fig. 1. In vitro lack of pDC development in cultures of Bcl11a-deficient fetal liver or adult bone marrow. (*A–D*) Fetal liver cells from *Bcl11a*$^{-/-}$, *Bcl11a*$^{+/-}$, and *Bcl11a*$^{+/+}$ mice were cultured in vitro with Flt3-L to induce the growth of cDC and pDC from progenitor cells. (*A*) Day 3 of culture (*Upper*) resulted in efficient production of cDCs (Cd11b^{+} Cd11c^{+}) among *Bcl11a*$^{+/+}$ and *Bcl11a*$^{+/-}$ genotypes, but a near absence of pDCs (Cd11b^{-} Cd11c^{+}) in the *Bcl11a*$^{-/-}$ homozygous knockout. Day 10 cultures (*Lower*) continued to exhibit this marked reduction in pDC generation (>10-fold compared with wild type). Results depicted are representative of $n = 3$ independent experiments. (*B*) Additional markers (B220, Ly6c) were used to track the outgrowth of cells in additional experiments ($n = 3$), confirming as above that only a minute portion of pDC-like cells (Cd11b^{-} Cd11c^{+}) could be detected in *Bcl11a*$^{-/-}$ cultures. (*C*) The pDC transcript Siglec-H was undetectable by RT-PCR in day 3 Flt3-L culture of *Bcl11a*$^{-/-}$ fetal liver progenitors. (*D*) *Bcl11a*$^{-/-}$ fetal liver culture (Flt3-L 7 d) failed to mount a measurable IFN-α response to type A CpG oligonucleotide (ODN D19) after 24 h of stimulation. (*E–J*) Adult bone marrow cells from pI:pC-treated *Bcl11a*$^{F/F}$*Mx1-cre*$^{YFP+}$ conditional knockout (cKO) mice or littermates (8 wk old) were cultured in vitro with Flt3-L to induce the growth of cDC and pDC from progenitor cells. (*E*) Flow cytometry of day 10 Flt3-L culture exhibited no pDC production from YFP^{+} (*Bcl11a*-deleted) bone marrow cells, whereas as shown in *F* the production of cDC was unimpeded and equivalent to control ($n = 3$ independent experiments). (*G* and *H*) Cultures of GM-CSF–supplemented cells (day 7) produced statistically similar frequencies of cDCs in both YFP^{+} (*Bcl11a*-deleted) and wild-type bone marrow. (*I*) Total cell numbers in Flt3-L cultures were drastically reduced (day 10; $P = 0.008$; Student *t* test), whereas total cells in GM-CSF stimulations were reduced only modestly (day 7; $P = 0.04$). (*J*) cDC-to-pDC ratios in Flt3-L–supplemented cultures were significantly different in YFP^{+} *Bcl11a*-deleted cells vs. total bone marrow cells (207.6 ± 87.7 vs. 3.05 ± 0.63, respectively, $P = 0.018$).

homozygous-deficient siblings. In addition to the previously documented loss of $B220^+$ B lymphocytes in these mice, we conjectured that $B220^+$ pDCs might also be absent from these tissues.

To test the role of Bcl11a in murine pDC development, we isolated hematopoietic cells from the fetal liver and spleen of *Bcl11a*$^{+/+}$, *Bcl11a*$^{+/-}$, and *Bcl11a*$^{-/-}$ E18 embryos. Examination of fetal organs was mandatory because constitutive homozygous deficiency of *Bcl11a* is neonatal lethal. In mouse, pDCs are $B220^+$ $Cd11c^+$ $Cd11b^-$, and express the specific marker Bst2/PDCA1/CD317. In $n = 3$ independent experiments, pDCs were missing from *Bcl11a*$^{-/-}$ KO mice. Collectively, the missing cells were $Cd11c^+$ $CD11b^-$ $Cd19^-$ RB6-8C5$^+$ $B220^+$ PDCA1$^+$. In one experiment, pDC were reduced 25-fold in the *Bcl11a* KO($^{-/-}$) compared with the wild-type littermate control ($^{+/+}$) (Fig. S1*B*).

We could not detect Siglec-H transcripts in *Bcl11a*$^{-/-}$ fetal liver precursors in vivo (Fig. S1*C*) or ex vivo (Fig. 1*C*), whereas Siglec-H expression was detectable in heterozygous and wild-type controls. Though immature pDCs (PDCA1$^-$) have been reported to be negative for Siglec-H transcripts, mature pDCs (PDCA1$^+$) are routinely positive for expression of this gene (18). In light of this observation, we could not exclude the possibility that pDC progenitors were blockaded at an intermediate stage of differentiation; this could result from cell-extrinsic Bcl11a-dependent effects modulated by accessory cells or the stromal milieu in general.

Bcl11a Is Required for Cytokine-Induced pDC Differentiation from Fetal Liver Progenitors in Vitro. The capacity of Bcl11a-deficient fetal liver cells to differentiate into pDCs was further investigated. *Bcl11a*$^{-/-}$ fetal liver cells were cultured in defined cytokine-supplemented media to reveal whether pDC precursors, which might persist in vivo, could be differentiated ex vivo. The development of pDCs and cDCs depends crucially on the hematopoietic cytokines Flt3-ligand (Flt3L) and GM-CSF in both human and mouse (10). Flt3L alone induces the growth of cDC and pDC in vitro from progenitor cells, and moreover, these are the only cell populations generated in Flt3L-supplemented bone marrow cultures (33). In contrast, GM-CSF exclusively promotes the differentiation of cDC from early hematopoietic progenitors and induces a single population of $Cd11c^+$ $Cd11b^+$ $B220^-$ cDCs, but not $Cd11c^+$ $Cd11b^-$ $B220^+$ pDCs, in culture (33).

In agreement with the observations made in vivo using KO mice, the ex vivo differentiation of *Bcl11a*$^{-/-}$ hematopoietic fetal-liver precursors failed to generate prototypical $Cd11c^+$ $Cd11b^-$ $Ly6c^+$ $B220^+$ pDCs in Flt3L-supplemented cultures (Fig. 1 *A* and *B*). *Bcl11a*$^{-/-}$ KO cultures consisted almost entirely of $Cd11c^{+/-}$ $Cd11b^+$ $B220^-$ myeloid cells and cDCs at all three time-points examined (days 3, 7, and 10). pDC and pDC-like cells that persisted were on average reduced >10-fold compared with cultures derived from littermate controls. In contrast to the profound impedance of pDC differentiation, *Bcl11a*$^{-/-}$ cDCs in Flt3L cultures appeared to differentiate fully, although clearly reduced in their relative percentage (Fig. 1 *A* and *B*). As reported in a recent study (9), cDC generation from *Bcl11a*$^{-/-}$ KO fetal precursors in control experiments using GM-CSF is abundant and unperturbed. The expression of PDCA1 was low among all Flt3L-derived pDCs, as previously documented (34), so the additional surface-marker Ly6c was included along with Cd11b, Cd11c, and B220 to track the outgrowth of cells using flow cytometry analysis. These cellular phenotypic profiles were confirmed in three independent experiments. Moreover, similar to RT-PCR of KO whole fetal liver, Siglec-H transcripts were undetectable among fetal liver precursors cultured in Flt3L for 3 d (Fig. 1*C*), underscoring the absence of this pDC-specific molecular program. The lack of a functional pDC phenotype in *Bcl11a*$^{-/-}$ mice was also supported by the lack of IFN-α production subsequent to stimulation of cultured cells with the type A CpG oligodeoxynucleotide D19, as determined by ELISA ($n = 1$) of culture supernatants (Fig. 1*D*).

Bcl11a Is Required for Cytokine-Induced pDC Differentiation from Adult Bone Marrow in Vitro. To determine whether the defect in fetal pDC development observed among Bcl11a-deficient conventional knockout mice is retained in adults, we constructed a floxed (F) allele of *Bcl11a* (Fig. S2 and *SI Text*). Our strategy results in deletion of the first exon, which is included in all previously characterized *Bcl11a* transcripts in mouse and man (2, 4, 35, 36). We crossed these mice to transgenic mice in which Cre recombinase is driven by the promoter of the *Mx-1* gene (37). The *Mx1-cre* transgene is expressed in hematopoietic stem cells (HSCs) and in all downstream lineages after induction with type I IFN or poly(I):poly(C) (pI:pC), allowing reliable deletion throughout the entire adult hematopoietic compartment. These mice were also crossed to a floxed STOP-YFP reporter mouse to positively identify the cells in which *Mx1*-Cre recombinase is activated.

Young adult (5 wk) *Bcl11a*$^{F/F}$*Mx1*-Cre*YFP*$^+$ mice underwent pI:pC induction, and bone marrow was collected at 8 wk for Flt3L and GM-CSF–supplemented cultures. In agreement with the observations made in vivo and ex vivo using KO mice, YFP^+ bone marrow precursors failed to generate $Cd11c^+Cd11b^-$ YFP^+ pDCs in Flt3L-supplemented cultures (Fig. 1*E*). To confirm phenotype, ∼75% of the $Cd11c^+CD11b^-$ pDCs in the control cultures were weakly positive for both PDCA-1 and Siglec-H. Interestingly, *Bcl11a*$^{F/F}$*Mx1*-Cre*YFP*$^+$ cultures consisted of substantial numbers of $Cd11c^{+/-}Cd11b^+$ MHC II^{hi} YFP^+ cDCs at day 10 (Fig. 1*F*), indicating a difference in cDC development between fetal and adult precursors. The cDC to pDC ratio was significantly altered in YFP^+ cells compared with total bone marrow in Flt3L supplemented cultures (Fig. 1*J*; 207.6 ± 87.7 to 3.05 ± 0.63, respectively, $P = 0.018$). In GM-CSF–supplemented cultures, cDCs differentiated normally and abundantly from YFP^+ bone marrow (Fig. 1 *G* and *H*). These cellular phenotypic profiles were confirmed in triplicate and in $n = 3$ independent experiments. Though total cell numbers were greatly reduced in Flt3L-supplemented cultures [15.8×10^6 vs. 3.43×10^6 in control and conditional KO (cKO), respectively], there was also mild reduction of total cells in GM-CSF–supplemented cultures (51.1×10^6 vs. 35.7×10^6 in control and cKO, respectively; Fig. 1*I*), indicating either a slight reduction in cDC development efficiency or possibly a reduction in cell survival.

Deletion of *Bcl11a* in Hematopoietic Precursors Results in a Robust Loss of pDCs but Spares Lin$^-$ Sca-1$^+$ c-kit$^+$ Progenitors, T cells, and cDCs. The floxed (F) allele of *Bcl11a* was crossed to transgenic mice in which Cre recombinase is driven by the promoter of the *Vav* gene (38). The *iVav-cre* transgene is expressed in HSCs and in all downstream lineages (39), allowing reliable deletion throughout the entire embryonic and adult hematopoietic compartment.

Young adult (6 wk) *Bcl11a*$^{F/F}$*Vav*-Cre mice consistently displayed a radical loss of B cells and pDCs in bone marrow, with a relative 10- to 50-fold reduction compared with control littermates ($n = 5$ independent experiments) as determined by PDCA1, CD11c, and B220 staining (Fig. 2*A*). The typical loss of B cells in any given experiment was observed to be proportional to the loss of pDCs, and the approximate B:pDC ratio of 10:1 typically observed in controls was also maintained in *Bcl11a*$^{F/F}$*Vav*-Cre knockout mice irrespective of the degree of cellular deletion in the bone marrow. An examination of the periphery resulted in a similar pairwise reduction of B cells and pDCs in the spleen (Fig. 2*A*); however, here the reduction was not as pronounced as in bone marrow. Importantly, splenic cDCs ($B220^-$ $CD11c^{high}$ $CD11b^+$ $MHCII^{high}$) were unaffected by *Bcl11a* deletion (Fig. 2*B*), as were $CD8^+$ or $CD8^-$ cDC subsets ($CD11c^+$ $CD8^+$ $CD11b^-$ $MHCII^+$ $B220^-$; $CD11c^+$ $CD8^+$ $CD11b^-$ $MHCII^{high}$ $B220^-$, respectively; Fig. 2*C*).

To determine whether dendritic cell precursors were impaired, bone marrow was stained for various lineage markers, including those that discriminate common myeloid progenitors (CMPs; Lin$^-$ $Flt3^+$ Sca-1$^-$ c-kit^{high} $CD115^+$) and CDPs (Lin$^-$ $Flt3^+$ Sca-1$^-$ c-kit^{lo}

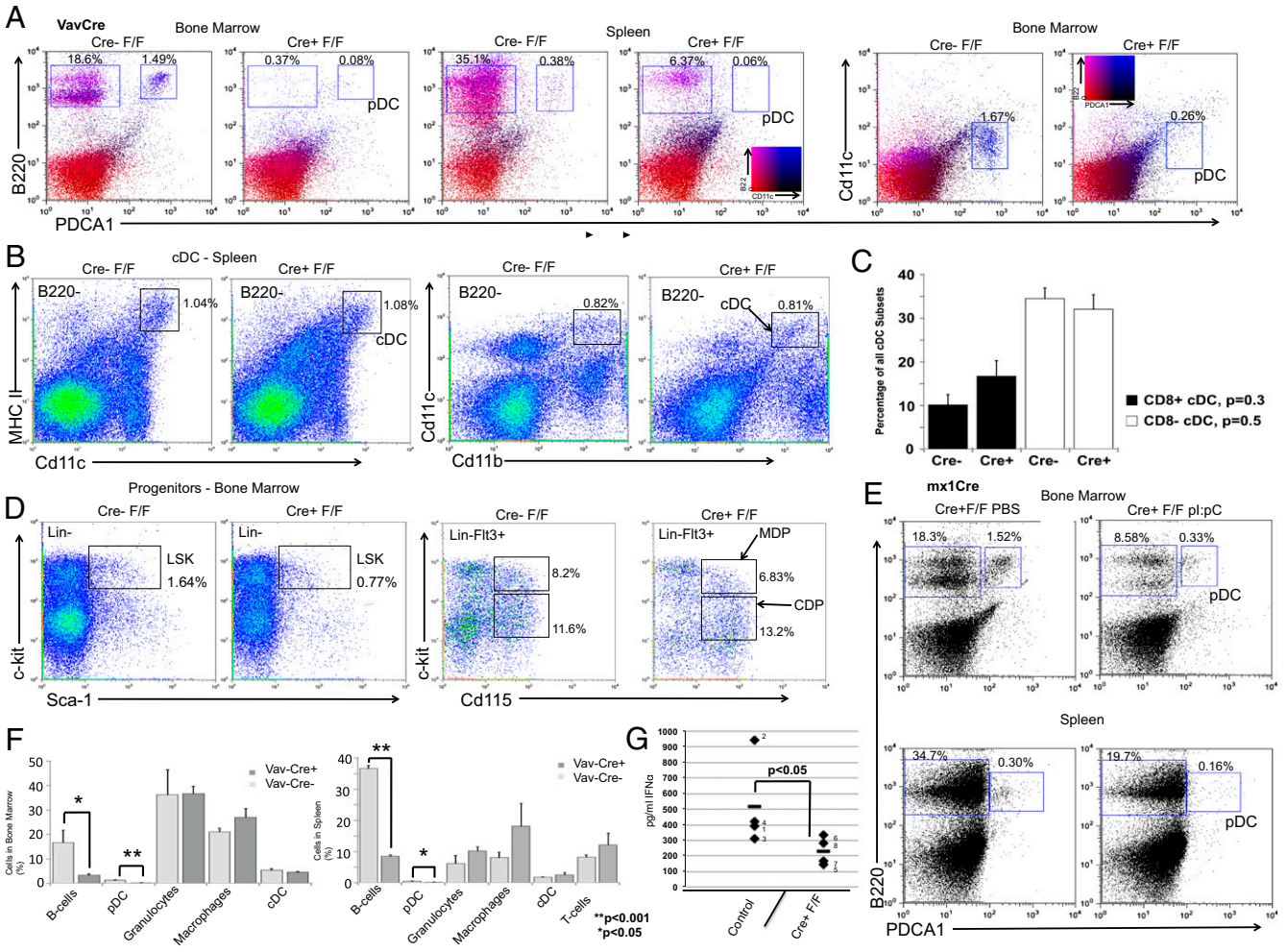

Fig. 2. Conditional elimination of *Bcl11a* in vivo leads to loss of pDC cellularity and function without perturbation of cDCs. (*A*) pDC are depleted in *Bcl11a* conditionally deleted adult mice. Homozygous *Bcl11a* cKO mice bearing *loxP*-flanked (F) targeted alleles (*Bcl11a*$^{F/F}$) were intercrossed with the *Vav*-Cre deleter C57/BL6 strain (*Vav*-Cre$^+$ F/F), which expresses Cre recombinase in HSC. Dot plot of B220$^+$ PDCA1$^+$ cells (*Left*) or Cd11c^{int} PDCA$^+$ cells (*Right*) shows a near complete loss of pDCs in the bone marrow of *Vav*-Cre$^+$ F/F mutants compared with littermate controls (10-fold to 50-fold loss; $n = 5$ independent experiments). The simultaneous loss of B220$^+$ PDCA1$^-$ B cells served as an internal control for Cre-mediated deletion efficiency. A similar loss of pDCs was confirmed in the spleen (*Center*), although the fold reduction (~fivefold) was not as pronounced as in bone marrow. (*B*) The generation of cDC (B220$^-$ MHC II^{hi} CD11c^{hi} CD11b$^+$) was unaffected by *Vav*-Cre–mediated knockout of *Bcl11a*. (*C*) The frequency of CD8$^+$ and CD8$^-$ cDC subsets in the spleen were statistically indistinguishable between *Vav*-Cre$^+$ F/F and controls. (*D*) Although fewer overall LSK progenitors were detected in *Vav*-Cre$^+$ F/F mice, both MDP and CDP progenitor populations persisted within the Flt3$^+$ compartment in cKO mice at percentages similar to controls. MDP (Lin$^-$ Flt3$^+$ Sca-1$^-$ CD115$^+$ c-kit^{hi}); CDP (Lin$^-$ Flt3$^+$ Sca-1$^-$ CD115$^+$ c-kit^{lo}). (*E*) pDC are also depleted in *Bcl11a*$^{F/F}$*Mx1*-Cre mice following induction of Cre-mediated deletion in HSC by treatment with pI:pC, but CDP and cDC are spared, analogous to results obtained with *Vav*-Cre deletion. (*F*) Hematopoietic lineages other than B and pDC were statistically unaffected in *Vav*-Cre$^+$ F/F mice relative to *Vav*-Cre$^-$ controls across independent experiments ($n = 3$; four per genotype) plotted as mean ± SEM (*$P < 0.05$; **$P < 0.001$; Student *t* test). (*G*) *Vav*-Cre$^+$ F/F mice are significantly impaired in type I IFN response to viral infection with ~1×10^7 pfu of human HSV strain 17 i.v. by tail-vein injection ($n = 1$; four per genotype) as measured by ELISA (232 ± 44.4 to 518 ± 144 pg/mL; data as means ± SEM; $P < 0.05$, Mann–Whitney, two-tailed test).

CD115$^+$; Fig. 2*D*). Consistent with a recent report (6), we observed an ~twofold reduction of Lin$^-$ Sca-1$^+$ c-kit$^+$ cells (LSK; Fig. 3*D*) in *Bcl11a*$^{F/F}$*Vav*-Cre bone marrow. However, neither macrophage-DC progenitor (MDP) nor CDP progenitor populations were substantially impaired in their relative percentages (Fig. 3*D*). Further, statistically similar relative percentages of cDCs (CD11c$^+$ CD11b$^+$ B220$^-$), granulocytes (Gr-1$^+$ CD11b$^+$), macrophages (CD11b$^+$ F4/80$^+$), and T cells (CD3ε$^+$ CD4CD8 DP and SP) were observed in bone marrow and spleen of cKO and control littermate mice (Fig. 2*E*). These observations are consistent with the original report (5) of conventional embryonic deletion of *Bcl11a* wherein B cells were selectively abolished yet T cells as well as myeloid and erythroid cells were preserved.

We confirmed these observations in the aforementioned *Bcl11a*$^{F/F}$*Mx1*-Cre adults following pI:pC-induced deletion (37). Here, too, B cells and pDCs were significantly reduced with little alteration of other cell populations (Fig. 2*F*). Except for the peculiar observation that T-cell absolute numbers are reduced exclusively among c-kit$^+$ precursor T cells when tamoxifen-inducible CreERT2 is used to induce a global deletion of *Bcl11a* exon 4 (6), our results are consistent with all prior data derived from conventional embryonic *Bcl11a*-deleted mice wherein approximately normal T-cell development occurs. Furthermore the *Mx1*-Cre data eliminate the possibility that this difference with our results derived from sparing of T cells of embryonic origin.

To investigate the ability of *Bcl11a*$^{F/F}$*Vav-cre* mice to produce type I IFN upon viral infection, we analyzed peripheral blood mononucleated cells of Cre-positive and Cre-negative littermates to assure expected phenotypes before delivering 1×10^7 pfu of human HSV strain 17 i.v. by tail-vein injection. As shown in Fig. 2*G*, serum

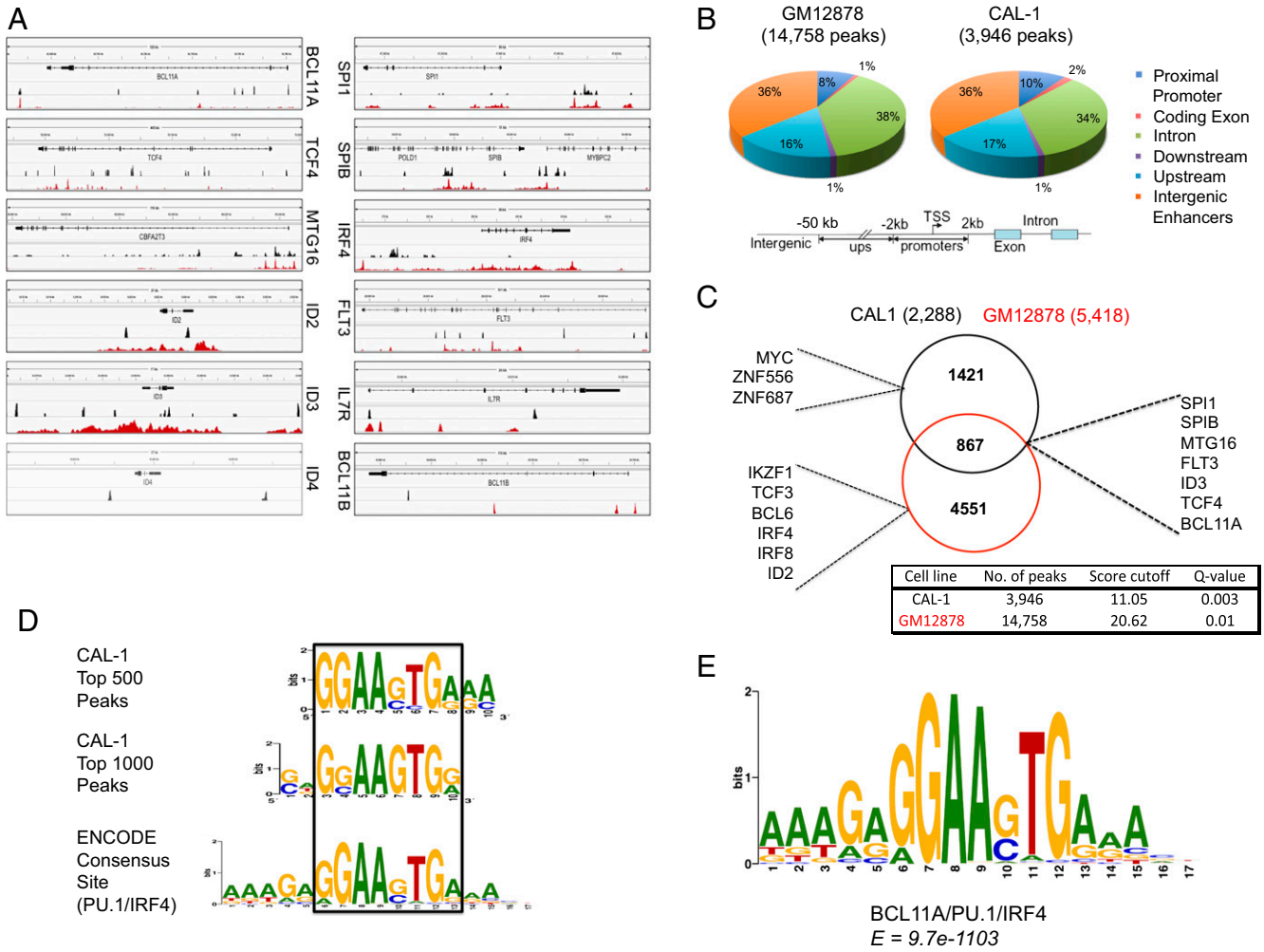

Fig. 3. ChIP-seq analysis of genome-wide BCL11A DNA binding in vivo. (*A*) Peak mapping along the loci of multiple pDC-related genes. ChIP-seq peaks from the CAL-1 human pDC (black, peak score ≥10) were determined and aligned with ENCODE Consortium ChIP-seq data for the human B lymphoblastoid cell line GM12878 (red, peak score ≥10). ID4 and the T-cell–specific paralogue, BCL11B, were chosen as negative controls because of their similarity to BCL11A and other IDs that contained highly correlated peaks. CAL-1 ChiP-seq resulted in smaller and fewer peaks than the ENCODE data (Fig. S3). (*B*) A pie chart representation of the distribution of BCL11A binding sites in six different genomic regions. Core promoters are within ±2 kb from the transcriptional start site (TSS); upstream is from 2 to 20 kb upstream from the TSS; and intergenic is a region not included as a promoter, upstream region, intron, or exon. The CAL-1 ChIP-seq peak distribution shows a striking similarity to that of the ENCODE Consortium's GM12878 cell line. (*C*) Overlap of BCL11A target genes between the two cell lines. A target gene was defined by a binding site occurring within 50 kb upstream through the intron of that gene. Analysis of the false discovery rate and associated Q-values were performed using Benjamini–Hochberg statistics. (*D*) De novo motif analysis from BCL11A ChIP-seq in CAL-1 cells. Alignment of the top 500 and top 1,000 CAL-1 ChIP-seq peaks show strong similarity to the top-ranked BCL11A ChIP-seq motif found in GM12878 cells, an EICE consensus site. (*E*) EICE motifs comprise the top-ranked BCL11A binding motifs in the GM12878 cell line. EICE is a previously identified composite DNA binding site for the Ets factor PU.1/SPI1 and for the IFN regulatory factor 4 (IRF4) that mediates cooperative binding of these factors to DNA. MEME analysis was used to calculate the expectation E-value for the occurrence of this motif within the GM12878 coincident peak sequences of BCL11A, PU.1/SPI1, and IRF4.

levels of IFN-α were markedly reduced 12 h postinjection in *Bcl11a*$^{F/F}$*Vav*-Cre mice compared with Cre-negative littermate controls (232 ± 88.9 to 518 ± 288 pg/mL, respectively). Thus, Bcl11a-deficient mice have a reduced capacity to generate this critical pDC mediator of the innate immune response.

Genome-Wide BCL11A Target Genes Include Previously Established Regulators of pDC Biology. ChIP-seq of the human CAL-1 cell line was used to identify genome-wide binding sites of BCL11A in pDCs. We found that BCL11A is recruited to the loci of several previously established pDC factors, including *SPI1*, *SPIB*, *E2-2/TCF4*, *IRF4*, *MTG16*, and *ID2*, and, interestingly, to its own proximal promoter region (Fig. 3*A*). The occupancy pattern of BCL11A in CAL-1 cells (within putative proximal promoters and intronic or intergenic loci) bore a striking resemblance to its binding distribution in the human EBV-transformed lymphoblastoid cell line (LCL) GM12878, based on published ENCODE Consortium data (www.factorbook.org/; Fig. 3*B*). Additionally, the top-ranked DNA binding motifs for the top CAL-1 and GM12878 binding sites were identical (Fig. 3 *D* and *E* and Fig. S4). Our data further suggest that some targets are bound in a cell-context dependent fashion (Fig. 3*C*). For example, whereas BCL11A was recruited to the same location in the *ID3* locus in both the B and pDC cell lines, its recruitment to the *ID2* locus was differential across the two lines. Ongoing studies of these and other cell-contextual patterns of BCL11A genomic binding are being confirmed in additional B-cell lines.

Evidence for a BCL11A-Regulated ID/E–Protein Interplay in Control of pDC Development. Recent findings have linked Id2 and Id3 regulation to differentiation of cDCs and pDCs via transcriptional inhibition of *E2-2/Tcf4* (24, 26, 40). Among our CAL-1 genome-wide

target genes we observed strong BCL11A binding to *ID3* (Fig. 3*A*). However, *ID2* peaks were weak and did not align with the relatively strong *ID2* peaks observed in GM12878 B cells (Fig. 3*A*). Using ChIP followed by endpoint PCR, we confirmed (n = 3) robust recruitment of BCL11A to the proximal promoter of *ID3* in chromatin prepared from the CAL-1 cell line, but not from an amplicon 10 kB upstream or from a cell line (Hodgkin lymphoma L428) negative for BCL11A expression (Fig. 4*B*). Additionally, the proximal promoter of *E2-2/TCF4* was also efficiently PCR amplified (n = 2) from CAL-1 chromatin (Fig. 4*B*). Within the ChIP regions of *ID3* and *E2-2* (base pairs –679 and –3762 upstream of their respective transcriptional start sites) reside evolutionarily conserved sequences (Fig. S4) that match the BCL11A binding consensus of Fig. 3*D*. In *ID3* this putative BCL11A binding site is positioned <100 bp downstream of a MspI/HpaII restriction site whose differential methylation has been correlated with myeloid vs.

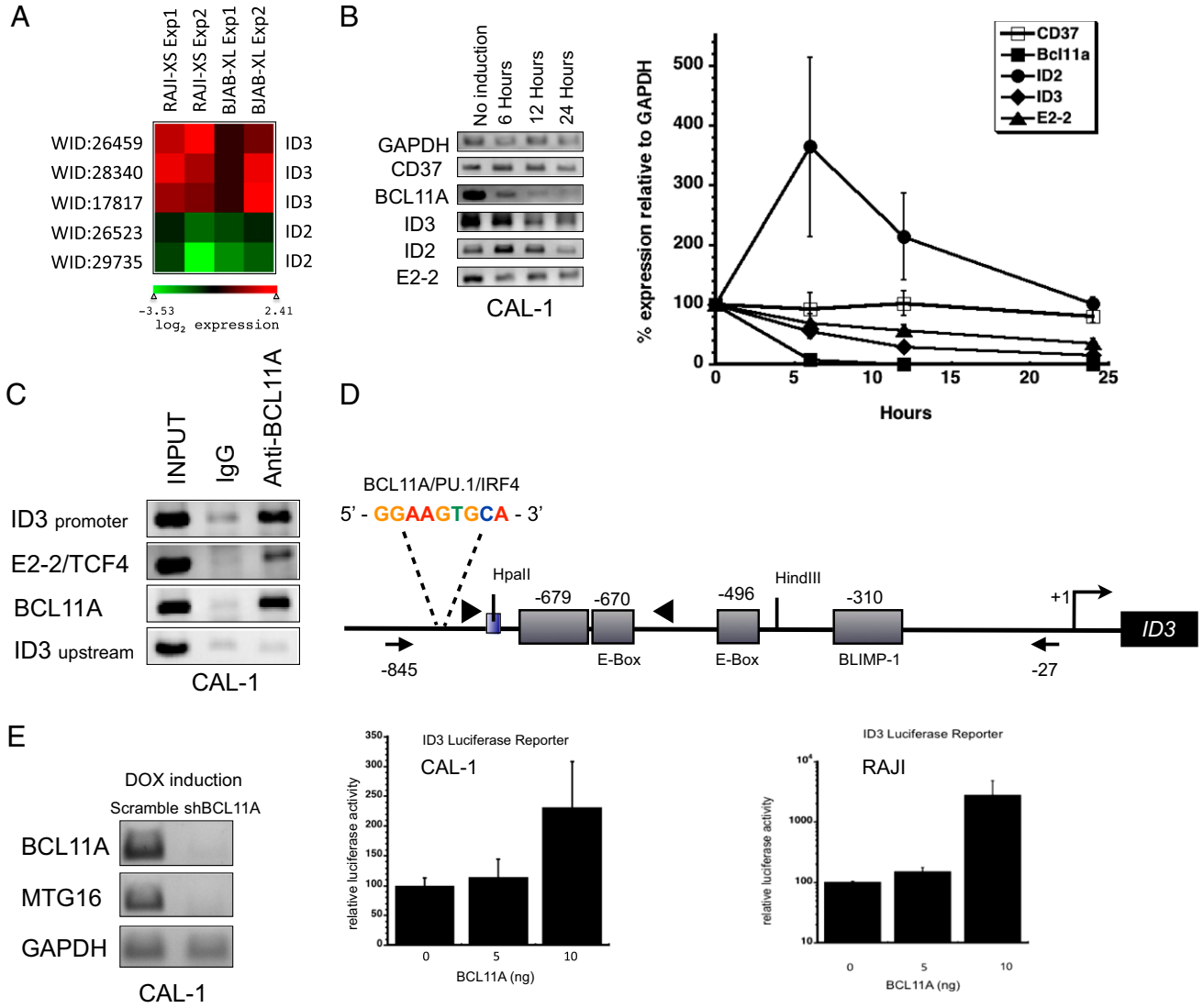

Fig. 4. BCL11A regulates ID2, ID3, MTG16, and E2-2/TCF4 in human B and pDC cell lines. (*A*) BCL11A isoforms (XS or XL) retrovirally overexpressed in Raji and BJAB Burkitt's lymphoma B-cell lines altered transcription (average threefold) of the HLH proteins *ID2* and *ID3* compared with mock-transduced control cells. Multiple (n > 4) independent experiments tracked by multiple probe elements spotted per LymphoChip cDNA microarray. (*B*) Inducible shRNA silencing of BCL11A down-regulates transcription of ID3 and E2-2. (*Left*) CAL-1 pDC cell line stably transduced with inducible shRNA targeted to exon 2 of Bcl11a under the control of a doxycycline (DOX)-inducible H1 promoter containing TETR binding sites (59). RT-PCR with optimal cycling conditions in the CAL-1 pDC cell line revealed strong knockdown of *BCL11A* transcripts beginning 6 h postinduction and continuing for >24 h. *ID3* and *E2-2* transcripts were correspondingly reduced throughout the 24-h experiment, whereas *ID2* was consistently, although transiently, induced; the irrelevant target gene *CD37* was unaffected. *GAPDH* amplification shows equivalence of mRNA amplification and loading. (*Right*) At 24 h, shRNA-mediated BCL11A knockdown resulted in *ID3* transcriptional inhibition >80%, and *E2-2* of 60%, when normalized to the *GAPDH* housekeeping control gene. Mean ± SD depicted; $n \geq 3$ experiments. (*C*) BCL11A is recruited to 5′ regulatory regions of *ID3*, *E2-2*, and itself. ChIP from CAL-1 human pDC cells using anti-BCL11A or control IgG antibodies was analyzed by endpoint PCR. Primers annealing 10 kb upstream of the ID3 TSS failed to amplify and thus served as a negative control. (*D*) Overexpression of BCL11A (XL) up-regulates ID3 promoter-driven reporter transcription in CAL1 pDCs and Raji B cells. (*Upper*) Schematic of the ID3 proximal promoter indicating the species-conserved EICE-like BCL11A DNA binding motif (Fig. S4); the location of BLIMP-1 and E-box motifs; and the HpaII methylation site. An 820-bp fragment spanning this region (indicated by arrows) that was consistently PCR amplified in ChIP experiments (indicated by wedges) was inserted upstream of luciferase in the pGL2 luciferase vector. (*Lower*) Dual luciferase activity was determined following transient transfection with increasing DNA levels (in nanograms) of the reporter into CAL1 human pDC cells or Raji B cells. Mean relative luciferase activity ± SEM obtained depicted; n = 2 independent experiments read in triplicate. (*E*) Knockdown of BCL11A results in MTG16 knockdown 24 h post-DOX induction in CAL-1 pDC cells.

lymphoid lineage choice (23) (Fig. 4*C*). Consistent with its absence in the CAL-1 ChIP-seq target list, we found no evidence for BCL11A recruitment to *ID2*. However, we confirmed binding of BCL11A to its own locus (Fig. 4*B*), raising the possibility that BCL11A is autoregulatory.

As an initial test of function, we overexpressed the major BCL11A isoform (XL) or a smaller, less well-characterized (4) isoform (XS) as retroviruses in Raji B cells. We observed that both BCL11A-XL and -XS strongly up-regulated *ID3* (average of 2.8- to 3.0-fold, respectively; Fig. 4*A*), whereas *ID2* was uniformly repressed (2.6- to 3.0-fold) by BCL11A-XL and -XS. Next, inducible short-hairpin RNA interference in CAL-1 pDC cells was used to specifically target a region (exon 2) common to all BCL11A isoforms. We observed a robust knockdown of *BCL11A* transcripts as well as a corresponding reduction in both *ID3* and *E2-2* transcripts at select time points (Fig. 4*C*). Knockdown of *BCL11A* was nearly absolute by the end of the first 24 h of shRNA induction. Assayed at the 24-h time point and normalized to the housekeeping control gene GAPDH, shRNA-mediated BCL11A knockdown resulted in an *ID3* transcriptional inhibition of over 80%, and *E2-2* of 60%, whereas the irrelevant target *CD37* was broadly unchanged. Direct *ID3* regulation was confirmed by BCL11A up-regulation of *ID3* promoter-driven luciferase activity in CAL1 and Raji (two- to 10-fold; Fig. 4*D*) transient transfections. Measurement at the earliest time point (6 h) showed, as expected, down-regulation of the direct E2-2 target gene, *ID2* (19). However, at subsequent time points (12 h, 24 h), *ID2* consistently and gradually returned to baseline levels, suggesting an indirect affect by BCL11A knockdown. As a potential mechanism, the ETO family corepressor *MTG16*, an established (41) negative regulator of *ID2* (41) and a BCL11A target gene (Fig. 3*A*), was virtually depleted upon *BCL11A* shRNA knockdown (Fig. 4*E*). Cell viability was similar among experimental and control groups at all time points. These results collectively support a model for ID/E–protein interplay regulated by BCL11A through its direct transcriptional activation of the pDC-essential gene *E2-2* and the E-protein antagonist *ID3*, while indirectly suppressing ID2 expression through direct activation of *MTG16*.

Discussion

BCL11A has an essential role in B-cell development (5) and B-cell malignancy (2). Recent reports have suggested a broader role for Bcl11a in HSC and lymphoid development (6). An additional role for BCL11A in pDC development had been implied only indirectly by microarray gene expression profiling (42, 43) and by the abundant presence of BCL11A protein in this cell type (44). Here, we establish experimentally a regulatory role for BCL11A in pDCs pivotal to their development and differentiation. We show that Bcl11a deficiency in vivo results in loss of both fetal and adult pDC, while sparing other lineages downstream of the HSC. We identify BCL11A-regulated target genes previously implicated as critical for pDC development (18, 27). Coupled with the recent finding (20) that *Bcl11a* is significantly up-regulated in CDPs, which exclusively give rise to pDCs and cDCs, our results strongly support a model for "pDC priming" (20, 45) in which differentiation into pDCs represents the default pathway for CDPs (readdressed below).

At present, all current evidence (6, 20) indicates that *Bcl11a* is expressed uniformly in the HSC compartment, even though this compartment comprises a heterogeneous collection of cells. There is no evidence for *Bcl11a* differential expression between lymphoid-primed vs. myeloid-primed stem cells or progenitors, so it is unexpected that *Bcl11a* deletion in HSCs would result in a pan–lymphoid-specific defect, while leaving myeloid cells unaffected. That hypothesis conflicts with the data obtained here and in the original report of embryonic germ-line *Bcl11a* deletion (5) in which only B cells (specifically $B220^+$ cells) were grossly affected. Conditional KO models produced by our group (promoter and exon 1 targeted deletion) and by Yu et al. (6) (exon 4 targeted deletion) reveal an approximate twofold reduction in LSKs, but, in the case of our model using hematopoietic-specific deletion, the relative fraction of GMP, MDP, and CDP are not affected; $CD8^+$ and $CD8^-$ cDC subsets are spared; and only B cells and pDCs are abolished. So clearly in addition to an effect on LSK hematopoiesis in general, there is a selective effect on CDP to pDC lineage development. In support of this selective effect, recent functional analyses (46) have provided compelling evidence that although BCL11A is expressed broadly among human HSCs and multilymphoid progenitors (MLPs)—which exhibit hybrid transcriptional states resembling stem, myeloid, and lymphoid programs extending across lineage-specific boundaries—the phenotype of silencing *BCL11A* in single-cell MLPs is consistent precisely with the phenotype of mice deficient in Bcl11a in which there is no B-cell development. The authors concluded that Bcl11a directs MLP commitment exclusively to the B-cell lineage and does not have a pan-lymphoid effect (46). Analogously, our data suggest that Bcl11a selectively directs CDP commitment to the pDC lineage.

The field of pDC biology has generally focused on adult progenitors isolated from bone-derived and adult-derived pDC progenitors. We and others have used fetal liver isolated from perinatally lethal *Bcl11a* null mice (5, 9) to confirm an absolute cellular, molecular, and functional absence of pDCs in the embryo. As with these observations, Esashi et al. (34) in their studies of the signal transducer STAT5 found that fetal liver pDCs were responsive to Flt3-L, supporting the hypothesis that fetal and adult pDC progenitors share a common developmental pathway. HSCs isolated from human fetal liver also give rise to pDC (47), suggesting that the same ontogenetic pathway is conserved in humans. This conclusion is further buttressed by the work here showing that *Bcl11a*, when eliminated conditionally in bone marrow HSCs, is equally critical to adult pDC development and function. In contrast to pDC development, an odd, merely partial defect in $Bcl11a^{-/-}$ cDC differentiation can be observed in vitro but only when fetal liver precursors are cultured with Flt3L (not GM-CSF; ref. 9; our data), whereas their development in vivo is unimpeded and persists normally whether cDC are derived from fetal precursors transplanted to adult chimeras (9) or from conditionally deleted adult precursors (our data). This finding indicates that cDC development is Bcl11a-independent.

Microarray profiling of the common lymphoid progenitor (CLP) or CMPs illustrated how, among 218 differentially expressed genes, *BCL11A* and *E2-2* are two key elements distinguishing the gene expression profile of human pDCs from cDCs (48). Furthermore, prior genome-wide analysis highlighted *BCL11A* and *E2-2* as key genes for pDC vs. cDC lineage discrimination conserved between mouse and human (13). Our results advance a model in which BCL11A regulates E2-2 activity by both direct and indirect mechanisms, suggesting a network through which BCL11A-driven pDC development might occur. We observed BCL11A-mediated modulation of both *ID2* and *ID3* transcription levels, and the recruitment of BCL11A to consensus DNA binding sites upstream of the promoters of *ID3* and of the pDC essential and specific transcription factor *E2-2*. *Bcl11a*-directed shRNA interference strongly reduced ID3, MTG16, and E2-2 expression, whereas ID2 expression was derepressed, albeit transiently. That ID2 modulation was observed in the absence of BCL11A is consistent with its direct repression by E2-2 (19). However, the reciprocal modulation of *BCL11A* (as well as *ID2*) by E2-2, as reported by Reizis and coworkers (19), adds a layer of complexity that seems to defy a simple linear network defining pDC specification. Nevertheless, our data in Bcl11a-deficient mice clearly demonstrate that this factor is necessary for the development of all mature pDCs. cDCs, which derive solely from the CDP, persist, indicating the lack of a requirement for BCL11A in development in these cells.

Because ID proteins antagonize E-protein activity, and E-proteins are essential to the development and differentiation of lymphocytes and pDCs (11, 18, 21), the identification of transcription factors capable of modulating ID expression immediately suggests mechanistic models for lineage determination. ID2 and ID3, in particular, have documented roles in murine and human B-cell, T-cell, and pDC biology, and modulate the developmental potential of CDPs and CLPs (23–30). Though both Id2 and Id3 are coexpressed in purified CDPs (40), only Id3 is detectable in CLPs (49), and notably, differential expression is maintained in the downstream cDC and pDC progeny where cDCs are strongly positive for Id2 but chiefly negative for Id3, and the opposite is true for pDC (40). We have uncovered a role for BCL11A in the transcriptional regulation of *ID3*, which calls to mind the related identification of *ID2* as a target gene repressed by BCL11B (50), a highly similar paralogue of BCL11A essential for T-cell development (2). The orchestration and maintenance of lymphoid cell fates through the timing and overall dosage of ID3 (and ID2) and the resulting antagonism of E2A function has been previously described (29, 30). Similar observations regarding gene dosage and dendritic cell commitment have also been previously described for the PU.1/SPI1 transcription factor (51). Collectively, these observations provide a paradigm for understanding how timing, dosage, and the distinct pairing preferences of individual ID proteins might determine various lineage commitments.

Additionally, it should be noted that the top-ranked BCL11A consensus DNA binding motif that we and others (ENCODE Consortium) have discovered is the same motif previously identified as an Ets transcription factor/interferon regulatory transcription factor (IRF) composite element (EICE). EICE is known to be dually occupied by one of the two Ets factors, PU.1/SPI1 or SPIB, in combination with one of the two IRF factors, IRF4 or IRF8 (51, 52). Other Ets/IRF factors do not interact in this fashion (53). Each of these four factors is known to be involved in pDC development or maintenance (45, 54), and we have previously confirmed that BCL11A drives both IRF4 and IRF8 expression in mouse pre-B cells (49, 55). That BCL11A is recruited to the loci of each of these genes in human pDC CAL-1 chromatin and to evolutionarily conserved EICE-like sites within the promoter regions of itself, ID3, and E2-2/TCF4, places BCL11A near the top of a pDC gene regulatory hierarchy (Fig. S4).

In conclusion, rather than linear opposition of a default cDC differentiation pathway exerted by E2-2, in part, through BCL11A-mediated repression (19), we propose instead a feedback loop between E2-2 and BCL11A that constitutively maintains pDC identity (Fig. S5). Our data suggest that in this loop, BCL11A is activating E2-2 transcription and that BCL11A induces transcription of ID3, which may in turn heterodimerize with and reduce the protein activity of E2-2 (or other E-protein family members). In this way, ID3 and, perhaps, BCL11A autoregulation, provide homeostatic maintenance within pDC by buffering E2-2. Conversely, *Id2*$^{-/-}$ mice display no loss of pDC (24), yet ID2 remains expressed (albeit at modest levels) in CDP but not in pDC (20, 40); this leads us to speculate that within the CDP, BCL11A fortifies the default pathway by E2-2–mediated down-regulation of the ID2 repressor while concurrently driving MTG16 expression, thereby reducing ID2 activity at the protein level (41). For ID2 to rise to levels that would push CDPs to cDCs, it must down-regulate E2-2, BCL11A, and the other default pathway genes that are increased during the commitment of MDP to CDP but not to monocytes (20). Accordingly, we observed cDC generation in *Bcl11a* cKO mice to be unaffected. In our model, loss of BCL11a reduces E2-2 and MTG16 levels, allowing a sufficient increase of ID2 mRNA and activity for normal cDC development from the CDP (Table S5).

Materials and Methods

Conventional *Bcl11a*$^{-/-}$ Mice. All housing, husbandry, and experimental procedures with *Bcl11a* knockout and control mice were approved by the Institutional Animal Care and Use Committees at The University of Texas at Austin. The generation of *Bcl11a*$^{-/-}$ mice has been previously described (5). Mice were routinely PCR genotyped using tail genomic DNA and two primer pairs at an annealing temperature of 65 °C (primers in Table S1).

Generation of *Bcl11a* cKO Mice. Full details are provided in *SI Text*.

Flow Cytometry. Analysis was performed on FACSCalibur or Fortessa flow cytometers (BD Biosciences) and analyzed using CellQuest (BD Biosciences), WinMDI (Scripps Research Institute), or FlowJo (Tree Star) software. Fetal liver and spleen were prepared from pups (E15–E18) taken by Cesarean section. Single-cell suspensions were incubated 15 min on ice with Fc Block (BD Biosciences) before staining with antigen-specific monoclonal antibodies (Table S2) in D-PBS/2% (vol/vol) FBS FACS buffer.

RT-PCR. Total RNA was extracted from *Bcl11a*$^{-/-}$ fetal liver cells (or Bcl11a cKO spleen cells) using TRIzol reagent (Invitrogen) and oligo-dT cDNA was prepared using SuperScript III First-Strand Synthesis System for RT-PCR (Invitrogen). Taq polymerase (New England Biolabs) and a Perkin-Elmer 2700 thermocycler were used to amplify transcripts for the following mouse genes: *Bcl11a*, *Siglech*, *Id3*, *Cd19*, *β-Actin*, *Hprt.* Primers listed in Table S1.

Culture of Fetal Liver or Bone Marrow Cells. Cells were cultured in 100 ng/mL Flt3L or 50 ng/mL GM-CSF to induce pDC or cDC expansion, respectively. Time points are indicated in text and figures. Details in *SI Text*.

Retroviral Transduction of B-Cell Lines and LymphoChip Gene Expression Profiling. Phoenix-A (ΦNX-A) amphotropic 293 cells were used to package retroviruses containing pXY-PURO (negative control vector) or pXY-BCL11A-XS or pXY-BCL11A-XL using Fugene-6 reagent (Roche). Retroviral supernatant was used to infect target cells. Following puromycin selection, cells were pelleted by centrifugation, media-aspirated, and the cells lysed in TRIzol reagent for total RNA extraction. RNA was used for LymphoChip microarray profiling (56) or oligo-dT cDNA synthesis using a SuperScript III reagent kit (Invitrogen) and for endpoint RT-PCR experiments. RT-PCR primers and cycling conditions are listed in Table S1.

ChIP and ChIP Followed by ChIP-seq. ChIP assays were performed as described (57). More details and the PCR primers used are listed in Table S1. For ChIP-seq, DNA was analyzed by deep sequencing using Illumina sequencing technology.

Inducible shRNA Knockdown and RT-PCR in the CAL-1 pDC Cell Line. CAL-1 cells were stably transduced with a retrovirus expressing the bacterial tetracycline repressor (TETR) and the blasticidin resistance gene, followed by retroviral transduction with a Phoenix-E packaged pRSMX-PG TETR-inducible vector containing shRNA targeted to exon 2 of Bcl11a (58). Doxycycline (50 μg/mL) was applied for induction of shRNA expression. Cells were harvested for total RNA isolation at multiple time points. RT-PCRs with the listed human primer pairs (Table S1) were performed to amplify gene transcripts from induced BCL11A knockdown cells.

HSV Challenge and IFN-α ELISA. *Vav*-Cre–deleted Bcl11a or cre-negative littermate or age-matched controls were infected with 1×10^7 pfu of HSV1 (ATCC) by tail-vein injection. Blood was collected at 6, 12, and 24 h post-injection by saphenous vein bleed, centrifuged at 10,000 × *g* for 10 min for serum collection, and frozen at −80 °C. Detection and quantification of serum IFN-α was performed by ELISA following manufacturer's protocol (eBioscience; Fig. 3*G*). Before infection, the expected phenotypic B and pDC deficiency in cre-deleted mice was confirmed by FACS (*SI Text*).

ACKNOWLEDGMENTS. We thank June V. Harriss, Deborah Surman, and the late Shanna D. Maika for expert assistance in the generation of *Bcl11a* conditional knockout mice, and Chhaya Das and Maya Ghosh for help in ChIP analysis and cell culture. The CAL-1 cell line was kindly provided by Dr. Takahiro Maeda and Dr. Boris Reizis. Conventional Bcl11a knockout mice were provided by Dr. Pentao Liu. Support for this work was provided by the Intramural Research Program of the National Institutes of Health (NIH) National Cancer Institute, Center for Cancer Research (to L.M.S. and A.L.S.); NIH Grants F32CA110624 (to G.C.I.) and R01CA31534 (to H.O.T.); Cancer Prevention Research Institute of Texas (CPRIT) Grants RP100612, RP120348; and the Marie Betzner Morrow Centennial Endowment (H.O.T).

1. Fell HP, Smith RG, Tucker PW (1986) Molecular analysis of the t(2;14) translocation of childhood chronic lymphocytic leukemia. *Science* 232(4749):491–494.
2. Satterwhite E, et al. (2001) The BCL11 gene family: Involvement of BCL11A in lymphoid malignancies. *Blood* 98(12):3413–3420.
3. Mitelman F, Johansson B, Mertens F (2004) Fusion genes and rearranged genes as a linear function of chromosome aberrations in cancer. *Nat Genet* 36(4):331–334.
4. Liu H, et al. (2006) Functional studies of BCL11A: Characterization of the conserved BCL11A-XL splice variant and its interaction with BCL6 in nuclear paraspeckles of germinal center B cells. *Mol Cancer* 5:18.
5. Liu P, et al. (2003) Bcl11a is essential for normal lymphoid development. *Nat Immunol* 4(6):525–532.
6. Yu Y, et al. (2012) Bcl11a is essential for lymphoid development and negatively regulates p53. *J Exp Med* 209(13):2467–2483.
7. Kustikova O, et al. (2005) Clonal dominance of hematopoietic stem cells triggered by retroviral gene marking. *Science* 308(5725):1171–1174.
8. Pelayo R, et al. (2005) Derivation of 2 categories of plasmacytoid dendritic cells in murine bone marrow. *Blood* 105(11):4407–4415.
9. Wu X, et al. (2013) Bcl11a controls Flt3 expression in early hematopoietic progenitors and is required for pDC development in vivo. *PLoS ONE* 8(5):e64800.
10. Wu L, Liu YJ (2007) Development of dendritic-cell lineages. *Immunity* 26(6):741–750.
11. Reizis B (2010) Regulation of plasmacytoid dendritic cell development. *Curr Opin Immunol* 22(2):206–211.
12. Swiecki M, Colonna M (2010) Unraveling the functions of plasmacytoid dendritic cells during viral infections, autoimmunity, and tolerance. *Immunol Rev* 234(1):142–162.
13. Robbins SH, et al. (2008) Novel insights into the relationships between dendritic cell subsets in human and mouse revealed by genome-wide expression profiling. *Genome Biol* 9(1):R17.
14. Colonna M, Trinchieri G, Liu YJ (2004) Plasmacytoid dendritic cells in immunity. *Nat Immunol* 5(12):1219–1226.
15. Shigematsu H, et al. (2004) Plasmacytoid dendritic cells activate lymphoid-specific genetic programs irrespective of their cellular origin. *Immunity* 21(1):43–53.
16. Wang YH, Liu YJ (2004) Mysterious origin of plasmacytoid dendritic cell precursors. *Immunity* 21(1):1–2.
17. Reizis B, Bunin A, Ghosh HS, Lewis KL, Sisirak V (2011) Plasmacytoid dendritic cells: Recent progress and open questions. *Annu Rev Immunol* 29:163–183.
18. Cisse B, et al. (2008) Transcription factor E2-2 is an essential and specific regulator of plasmacytoid dendritic cell development. *Cell* 135(1):37–48.
19. Ghosh HS, Cisse B, Bunin A, Lewis KL, Reizis B (2010) Continuous expression of the transcription factor e2-2 maintains the cell fate of mature plasmacytoid dendritic cells. *Immunity* 33(6):905–916.
20. Miller JC, et al.; Immunological Genome Consortium (2012) Deciphering the transcriptional network of the dendritic cell lineage. *Nat Immunol* 13(9):888–899.
21. Kee BL (2009) E and ID proteins branch out. *Nat Rev Immunol* 9(3):175–184.
22. Lin YC, et al. (2010) A global network of transcription factors, involving E2A, EBF1 and Foxo1, that orchestrates B cell fate. *Nat Immunol* 11(7):635–643.
23. Deed RW, Jasiok M, Norton JD (1998) Lymphoid-specific expression of the Id3 gene in hematopoietic cells. Selective antagonism of E2A basic helix-loop-helix protein associated with Id3-induced differentiation of erythroleukemia cells. *J Biol Chem* 273(14): 8278–8286.
24. Hacker C, et al. (2003) Transcriptional profiling identifies Id2 function in dendritic cell development. *Nat Immunol* 4(4):380–386.
25. Jaleco AC, et al. (1999) Genetic modification of human B-cell development: B-cell development is inhibited by the dominant negative helix loop helix factor Id3. *Blood* 94(8):2637–2646.
26. Ji M, et al. (2008) Id2 intrinsically regulates lymphoid and erythroid development via interaction with different target proteins. *Blood* 112(4):1068–1077.
27. Spits H, Couwenberg F, Bakker AQ, Weijer K, Uittenbogaart CH (2000) Id2 and Id3 inhibit development of CD34(+) stem cells into predendritic cell (pre-DC)2 but not into pre-DC1. Evidence for a lymphoid origin of pre-DC2. *J Exp Med* 192(12):1775–1784.
28. Nagasawa M, Schmidlin H, Hazekamp MG, Schotte R, Blom B (2008) Development of human plasmacytoid dendritic cells depends on the combined action of the basic helix-loop-helix factor E2-2 and the Ets factor Spi-B. *Eur J Immunol* 38(9):2389–2400.
29. Miyazaki M, et al. (2011) The opposing roles of the transcription factor E2A and its antagonist Id3 that orchestrate and enforce the naive fate of T cells. *Nat Immunol* 12(10):992–1001.
30. Jones-Mason ME, et al. (2012) E protein transcription factors are required for the development of CD4(+) lineage T cells. *Immunity* 36(3):348–361.
31. Loveys DA, Streiff MB, Kato GJ (1996) E2A basic-helix-loop-helix transcription factors are negatively regulated by serum growth factors and by the Id3 protein. *Nucleic Acids Res* 24(14):2813–2820.
32. Roberts EC, Deed RW, Inoue T, Norton JD, Sharrocks AD (2001) Id helix-loop-helix proteins antagonize pax transcription factor activity by inhibiting DNA binding. *Mol Cell Biol* 21(2):524–533.
33. Gilliet M, et al. (2002) The development of murine plasmacytoid dendritic cell precursors is differentially regulated by FLT3-ligand and granulocyte/macrophage colony-stimulating factor. *J Exp Med* 195(7):953–958.
34. Esashi E, et al. (2008) The signal transducer STAT5 inhibits plasmacytoid dendritic cell development by suppressing transcription factor IRF8. *Immunity* 28(4):509–520.
35. Sankaran VG, et al. (2009) Developmental and species-divergent globin switching are driven by BCL11A. *Nature* 460(7259):1093–1097.
36. Xu J, et al. (2010) Transcriptional silencing of gamma-globin by BCL11A involves long-range interactions and cooperation with SOX6. *Genes Dev* 24(8):783–798.
37. Kühn R, Schwenk F, Aguet M, Rajewsky K (1995) Inducible gene targeting in mice. *Science* 269(5229):1427–1429.
38. Georgiades P, et al. (2002) VavCre transgenic mice: A tool for mutagenesis in hematopoietic and endothelial lineages. *Genesis* 34(4):251–256.
39. Stadtfeld M, Graf T (2005) Assessing the role of hematopoietic plasticity for endothelial and hepatocyte development by non-invasive lineage tracing. *Development* 132(1):203–213.
40. Felker P, et al. (2010) TGF-beta1 accelerates dendritic cell differentiation from common dendritic cell progenitors and directs subset specification toward conventional dendritic cells. *J Immunol* 185(9):5326–5335.
41. Ghosh HS, Liu K, Hiebert S, Reizis B (2012) Eto2/MTG16 regulates E-protein activity and subset specification in dendritic cell development. *Blood* 120(21). Available at https://ash.confex.com/ash/2012/webprogram/Paper53299.html.
42. Su AI, et al. (2004) A gene atlas of the mouse and human protein-encoding transcriptomes. *Proc Natl Acad Sci USA* 101(16):6062–6067.
43. Shaffer AL, et al. (2006) A library of gene expression signatures to illuminate normal and pathological lymphoid biology. *Immunol Rev* 210:67–85.
44. Pulford K, et al. (2006) The BCL11AXL transcription factor: Its distribution in normal and malignant tissues and use as a marker for plasmacytoid dendritic cells. *Leukemia* 20(8):1439–1441.
45. Satpathy AT, Murphy KM, Kc W (2011) Transcription factor networks in dendritic cell development. *Semin Immunol* 23(5):388–397.
46. Laurenti E, et al. (2013) The transcriptional architecture of early human hematopoiesis identifies multilevel control of lymphoid commitment. *Nat Immunol* 14(7):756–763.
47. Blom B, Ho S, Antonenko S, Liu YJ (2000) Generation of interferon alpha-producing predendritic cell (Pre-DC)2 from human CD34(+) hematopoietic stem cells. *J Exp Med* 192(12):1785–1796.
48. Ishikawa F, et al. (2007) The developmental program of human dendritic cells is operated independently of conventional myeloid and lymphoid pathways. *Blood* 110(10):3591–3660.
49. Boos MD, Yokota Y, Eberl G, Kee BL (2007) Mature natural killer cell and lymphoid tissue-inducing cell development requires Id2-mediated suppression of E protein activity. *J Exp Med* 204(5):1119–1130.
50. Li P, et al. (2010) Reprogramming of T cells to natural killer-like cells upon Bcl11b deletion. *Science* 329(5987):85–89.
51. Carotta S, Wu L, Nutt SL (2010) Surprising new roles for PU.1 in the adaptive immune response. *Immunol Rev* 238(1):63–75.
52. Glasmacher E, et al. (2012) A genomic regulatory element that directs assembly and function of immune-specific AP-1-IRF complexes. *Science* 338(6109):975–980.
53. Escalante CR, et al. (2002) Crystal structure of PU.1/IRF-4/DNA ternary complex. *Mol Cell* 10(5):1097–1105.
54. Tamura T, et al. (2005) IFN regulatory factor-4 and -8 govern dendritic cell subset development and their functional diversity. *J Immunol* 174(5):2573–2581.
55. Lee BS, et al. (2013) The BCL11A transcription factor directly activates RAG gene expression and V(D)J recombination. *Mol Cell Biol* 33(9):1768–1781.
56. Alizadeh A, et al. (1999) The LymphoChip: A specialized cDNA microarray for the genomic-scale analysis of gene expression in normal and malignant lymphocytes. *Cold Spring Harb Symp Quant Biol* 64:71–78.
57. Lee BK, Bhinge AA, Iyer VR (2011) Wide-ranging functions of E2F4 in transcriptional activation and repression revealed by genome-wide analysis. *Nucleic Acids Res* 39(9): 3558–3573.
58. Ngo VN, et al. (2006) A loss-of-function RNA interference screen for molecular targets in cancer. *Nature* 441(7089):106–110.